UNDERSTANDING THE SPACE WEATHERING OF MERCURY THROUGH LABORATORY EXPERIMENTS. M. S. Thompson[1], K. E. Vander Kaaden[2], M. J. Loeffler[3], and F. M. McCubbin[4]. [1]Department of Earth, Atmospheric, and Planetary Sciences, Purdue University, West Lafayette, IN, 47907, (mthompson@purdue.edu) [2]Jacobs, NASA Johnson Space Center, Houston, TX, 77058, [3]Northern Arizona University, Flagstaff, AZ, 86011, [4]ARES, NASA Johnson Space Center, Houston, TX, 77058.

Introduction: Airless surfaces across the solar system are continually modified by energetic particles from solar wind and micrometeoroid bombardment [1,2]. This process is known as space weathering, and it alters the chemical, microstructural, and optical properties of surface regoliths on airless bodies, including Mercury. On the Moon and S-type asteroids, the reflectance spectral signatures of space weathering include reddening (increasing reflectance with increasing wavelength), darkening (lowering of reflectance), and the attenuation of characteristic absorption bands [2]. Such spectral changes are driven by the production of Fe-bearing nanoparticles (npFe) through both solar wind irradiation and micrometeoroid bombardment.

While our understanding of space weathering for the Moon and near-Earth S-types asteroids is advanced, insight into how these processes operate on other planetary bodies is limited. In particular, Mercury experiences a uniquely intense space weathering environment than planetary counterparts at 1 AU, including a more intense solar wind flux and higher velocity micrometeoroid impacts [4]. Additionally, Mercury has a surface composition unique in the inner solar system, including regions of the surface with very low albedo known as the low reflectance material (LRM), which is enriched in carbon, likely graphite, up to 4 wt.% [5]. In addition, the concentration of Fe across Mercury's surface is low (<2 wt.%) compared to the Moon or S-type asteroids asteroids [6]. Our understanding of the effects of space weathering on C-rich and Fe-poor phases is limited. Since Fe plays a critical role in the development of space weathering characteristics on other airless surfaces (e.g., npFe), its limited availability may significantly affect the development of space weathering features in Mercury surface materials.

We can simulate space weathering processes in the laboratory to explore their effects on the microstructural, chemical, and spectral characteristics of Mercury surface materials [7]. Here we used pulsed laser irradiation to simulate the short duration, high-temperature events associated with micrometeoroid impacts. We performed coordinated analyses including reflectance spectroscopy and electron microscopy to investigate the spectral, chemical, and microstructural changes in these mercurian analog samples.

Methods: For these experiments, we used forsteritic olivine with varying FeO contents, a mineral phase proposed to be abundant on the surface of Mercury. We mixed each sample with graphite to simulate LRM regions of the surface. We synthesized the olivine samples at 1-bar at NASA's Johnson Space Center and prepared pressed powder pellets for laser irradiation [8]. We prepared three samples, each with a base layer of olivine to maintain structural integrity and topped with a surface layer containing the graphite-olivine mixture: 1) Sample SC-001 San Carlos olivine (Fo90.91), 2) Sample F-S-002 with 0.05 wt.% FeO olivine, and 3) F-T-004 with 0.53 wt.% FeO olivine. Each sample was mixed with 5 wt.% powdered graphite and had grain sizes ranging from 45 to 125 μm. We irradiated each sample using a pulsed Nd-YAG laser, (λ=1064 nm, ~6 ns pulse duration, energy of 48 mJ/pulse) while under vacuum at Northern Arizona University. The laser was rastered 1x and then 5x over the surface of each sample to simulate progressive space weathering. We collected *in situ* reflectance spectra from the samples after each laser pulse with a Nicolet IS50 Fourier-Transform Infrared spectrometer (λ from 0.65-2.5 μm). We used an FEI Nova NanoSEM200 scanning electron microscope (SEM) and a Hitachi TM4000 Plus benchtop SEM at Purdue University to image the surface morphology and topography of the samples. We extracted thin sections for analysis in the transmission electron microscope (TEM) using the FEI Helios NanoLab 660 focused ion beam (FIB) SEM at the University of Arizona. We performed analysis of the microstructural and chemical characteristics of the samples using the 200 keV JEOL 2500 scanning TEM at Johnson Space Center.

Reflectance Spectroscopy Results: Reflectance spectra for each sample are shown in Fig. 1.

SC-001: The spectrum of the unirradiated sample exhibits a weak 1.0 μm absorption feature, associated with Fe^{2+} in the olivine, and low overall reflectance (Fig. 1a). The reflectance and the depth of the absorption band increases after 1x laser raster but are at their lowest after 5x laser rasters.

F-T-004: The unirradiated sample has a blue-sloped spectrum with low reflectance without identifiable absorption features (Fig. 1b). With progressive laser irradiation, the sample reflectance increases and becomes strongly red-sloped.

F-S-002: The unirradiated sample exhibits a dark, blue-sloped spectrum. The brightness of the sample increases

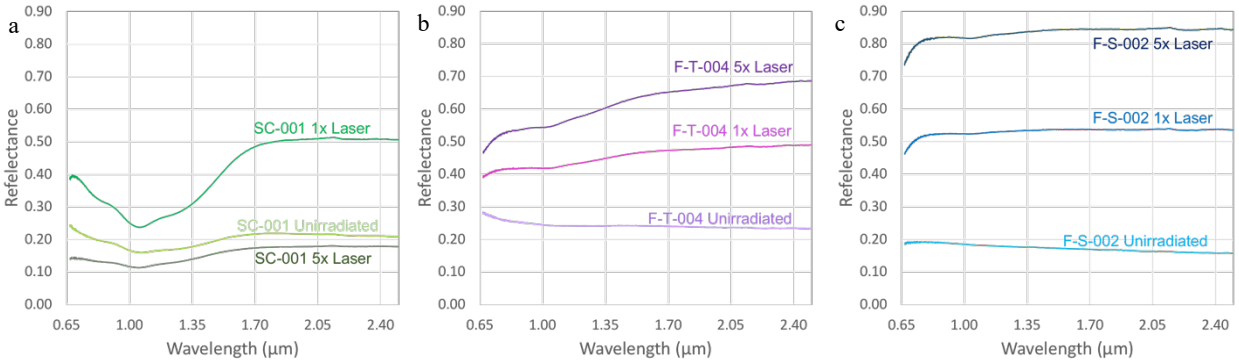

Figure 1: Reflectance data for the a) San Carlos olivine, b) F-T-004, and c) F-S-002 samples showing spectra for unirradiated material, after 1x laser shot, and after 5x laser shots. All spectra are presented on same reflectance scale.

significantly from <0.2 average reflectance over >0.8 reflectance in the most irradiated sample and the spectral slope also becomes slightly reddened (Fig. 1c).

Microstructural and Chemical Analysis: Two primary alteration textures were observed in the samples exposed to simulated space weathering: 1) fluffy C-rich, and 2) vesiculated melt. The fluffy C-rich texture is composed of low-density deposits distributed across the surface of the sample (Fig. 2A). Analysis of a FIB section extracted from a low-density C-rich region in sample SC-001 reveals multiple globule-type deposits, discrete from stacked graphite, likely produced via melting from the laser irradiation [9].

The vesiculated melt texture is smooth and uniformly distributed across isolated regions of the sample surface. The vesicles measure up to 100s of nm in diameter. Analysis of a FIB section from this texture was extracted from sample F-T-004 reveals a layer of amorphous melt material, close to 100 nm thick and uniform across the FIB section (Fig. 2B). Isolated regions of this melt layer contain small nanoparticles, <5 nm in diameter. Chemical analysis through energy dispersive X-ray spectroscopy reveals the composition of this layer is enriched in Si and depleted in Mg and O compared to the underlying sample.

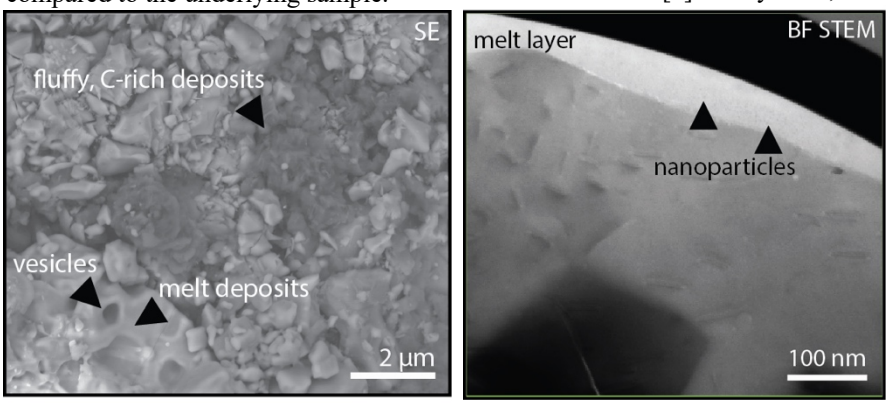

Figure 2: a) Secondary electron (SE) images of the surface morphology of the F-T-004 sample showing the vesiculated melt texture. B) Bright field (BF) scanning TEM (STEM) image showing the melt deposit and nanoparticles in sample F-T-004.

Implications for Space Weathering on Mercury: Previous experiments simulating space weathering of Mercury have shown darkening and reddening of spectra [7,10]. However, our use of low-Fe materials and graphite to create a sample set more analogous to the mercurian surface. Our results indicate that sample composition plays a significant and important role in the space weathering of Mercury. In particular, our spectral data demonstrates a strong correlation between spectral slope, Fe content, and simulated space weathering. While the variation in FeO content between samples F-S-002 and F-T-004 is <0.6 wt.%, the spectra deviate from flat to strongly red-sloped (F-T-004). This reddening may be linked to the presence of very small nanoparticles observed in the melt textures extracted from sample F-T-004. For the SC-001 sample, the fluffy C-rich textures may be developed by the amalgamation of small graphite particles into these unique morphologies. Such observations indicate that space weathering on Mercury may result in both familiar and new microstructural and chemical characteristics.

References: [1] Hapke B. (2001) *J. Geophys. Res.-Planet., 106,* 10039–10073. [2] Pieters C.M. and Noble S.K. (2016) *J. Geophys. Res-Planet., 121,* 1865–1884. [3] Lucey P.G., and Riner, M.A. (2011) *Icarus,* 212, 451-462. [4] Cintala M.J. (1992) *J. Geophys. Res.-Planet., 97,* 947–973. [5] Klima R.L. et al. (2018) *Geophys. Res. Letters*, *45*, 2945–2953. [6] Nittler L.R., et al. (2011) *Science 333,* 1847-1850. [7] Sasaki S. and Kurahashi E. (2004) Space weathering on Mercury, *Adv. Space Res.*, 33, 2152-2155. [8] Vander Kaaden K.E., et al. (2018) *LPSC XLIX,* Abstract 1230. [9] McGlaun M.L. et al. (2019) *LPSC L,* Abstract 2019. [10] Trang D. et al. (2018) *LPSC XLIX,* Abstract 2083.